Journal of the Korean Crystal Growth and Crystal Technology
Vol. 14, No. 3 (2004) 95-100

Effects of elastic strain on the agglomeration of silicide films for electrical contacts in integrated circuit applications

J.H. Choy†

Department of Physics, Simon Fraser University, Canada

(Received April 1, 2004)
(Accepted May 28, 2004)

Abstract This paper reports a potential problem in the electrical performance of the silicide film to silicon contacts with respect to the scaling trend in integrated circuit (IC) devices. The effects of elastic strain on the agglomeration of the coherent silicide film embedded in an infinite matrix are studied employing continuum linear elasticity and finite-difference numerical method. The interface atomic diffusion is taken to be the dominant transport mechanism where both capillarity and elastic strain are considered for the driving forces. Under plane strain condition with elastically homogeneous and anisotropic system with cubic symmetry, the dilatational misfit and the tetragonal misfit in the direction parallel to the film thickness are considered. The numerical results on the shape evolution agree with the known trend that the equilibrium aspect ratio of the film increases with the elastic strain intensity. When the elastic strain intensity is taken to be only a function of the film size, the flat film morphology with a large aspect ratio becomes increasingly unstable since the equilibrium aspect ratio decreases, as the film scales. The shape evolution results in a large decrease in contact to silicon area, and may deteriorate the electrical performances.

Key words Silicide, Electrical contact, Elastic strain, Epitaxy, Coherent

1. Introduction

The technology development trend in integrated circuit (IC) devices including both memory and non-memory applications dictates that the minimum feature size shrinks 11% annually. Although this trend is expected to continue in the next 15 years, the worldwide semiconductor associations forecast many aspects of the technologically challenging problems in order to overcome 100 nm barrier [1]. Among the issues regarding performance optimization as device scales, there is the increase in metal to silicon (Si) contact resistance as the contact size shrinks. Besides the size, the stability of the low resistive silicide/silicon interface at contact bottom is also an important factor contributing to the electrical contact resistance. Figure 1 depicts the device scaling trend for the next 12 years [1]. Since the scaling of the device, or the minimum feature size(designated by the minimum half pitch, and normally refers to [line width +space]/2 of the metal with minimum width) accompanies the scaling of the junction depth as well, the silicide film which must form within the junction at contact must scale its thickness in order to maintain the leakage current small across the junction. On the other hand, the silicide film aspect ratio, β_t (= contact size to film thickness) is observed to remain almost unchanged despite the scaling. The above scaling rule for the silicide film also applies to drain junctions in self-aligned silicide process (SALICIDE) [2, 3].

Normally the silicide film is formed by the deposition of the source metal on the desired silicon area, followed by the proper thermal annealing to ensure the reaction between the metal and Si to take place to produce the silicide. For the widely-used tungsten/titanium nitride/titanium (W/TiN/Ti) contact process, the reaction product is the low resistive (ρ = 13~16 μ ohm-cm) [4] orthorhombic C54 phase $TiSi_2$. The TiN liner protects Ti against fluorine (F) attack coming from WF_6 during tungsten deposition. The abnormal increase in contact resistance due to film agglomeration upon thermal annealing in dynamic random access memory (DRAM) device process has been reported earlier [5]. In SALICIDE process, $CoSi_2$ (ρ = 18~20 μ ohm-cm) [4] is know to be advantageous over $TiSi_2$ in forming the silicide upon device scaling [3].

In an effort to enhance the thermal stability and electrical performance, the epitaxial silicide film growth on Si substrate has been extensively studied for years [6-10]. $CoSi_2$ film, with atomic misfit ~1.2 %, appears to match relatively well with both Si (111) and (001), while $TiSi_2$ epitaxy on Si (111) is reported. The study on the stability and coarsening of these epitaxially

†Corresponding author
Tel: +604-291-4082
Fax: +604-291-3592
E-mail: junhoc@sfu.ca

grown films must take the atomic misfit-induced elastic strain into account. For an isolated particle coherently embedded in an infinite matrix with no mutual solubility, the relative intensity of the elastic strain to capillary force scales with the particle size since the elastic strain energy and the interfacial energy are proportional to the volume and area of the particle, respectively [11-13]. As a result, the equilibrium shape should be given by the function of the particle size. Obviously, the theory also applies to the thin film silicides in IC devices, which scales its dimension. The objective of the present study is to examine the effects of elastic strain on the thermal stability of the silicide films for contacts and drain junctions, as they become smaller in size. The 2-dimensional shape evolution of the film will be modeled using a finite-difference method assuming plane strain condition. The numerical tool originally developed by Voorhees *et al.* [11] will be modified to account for the interfacial diffusion in thin films.

2. Model

Assuming a sufficiently small elastic displacement, we employ continuum linear elasticity in describing the elastic strain field associated with atomic misfit. For a Cartesian coordinate system, Hooke's law dictates the linear relationship between stress, σ_{ij} and strain, e_{kl} with proportionality constant C_{ijkl} being the elastic stiffness tensor. We employ Einstein suffix notation where the repeated suffixes are to be summed over the values 1, 2, and 3, and a comma denotes differentiation with respect to the coordinates x_1, x_2, and x_3. For a crystal with cubic symmetry whose cube axes are parallel to the coordinates, 3 independent elastic constants in matrix notation are C_{11}, C_{12} and C_{44}. The elastic anisotropy factor, A_r is given by, $A_r = 2C_{44}/[C_{11} - C_{12}]$. For an isotropic material ($A_r = 1$), the shear modulus, μ is equal to C_{44}. For an anisotropic case, Hill's shear modulus [14] may be

Table 1
Elastic constants of single crystal Si [15], $CoSi_2$ [16] and $TiSi_2$ [17]. Only Hill's shear modulus is listed for orthoromic (C54) $TiSi_2$. The unit for the elastic constants is $1{\times}10^{11}$ Pa. The anisotropy factor is defined, $A_r = 2C_{44}/[C_{11} - C_{12}]$

	Si	$CoSi_2$	$TiSi_2$
C_{11}	1.68	2.28	1.40
C_{12}	0.65	1.40	
C_{44}	0.80	0.83	
μ_H	0.67	0.64	
A_r	1.56	1.89	

used for relative stiffness of the material. When $A_r > 1$, <100> becomes the elastically soft direction as $E_{100} < E_{110} < E_{111}$, where E is the Young's modulus. Table 1 lists the elastic constants and anisotropy factors of Si [15], $CoSi_2$ [16], and orthorhombic $TiSi_2$ [17] single crystals. In terms of shear modulus, Si and $CoSi_2$ are almost identical, while $TiSi_2$ is twice as stiff as the substrate. The present model employs the elastic constants and anisotropy close to those of cubic $CoSi_2$ with $A_r = 2$.

In modeling the shape evolution, we use the solution for an isolated and coherently misfiting silicide film embedded in an infinite Si substrate. With respect to the actual silicide structure of the IC devices, this approximation may be realized by considering a half part of the 2-fold symmetrical film geometry under the assumption that the surrounding liner metal has the elastic properties identical to those of Si substrate. Although the problem is over-simplified, the solutions thus obtained are expected to show clearly the effects of elastic strain. Both the film and Si are assumed to be elastically homogeheous, and have cubic symmetry. At the film/substrate/liner metal triple junction, the contact angle is taken to be 90° so that the film/liner metal interface becomes the mirror plane. The mutual solubility between the two phases is ignored so that the constant volume condition may hold. For a 2 dimensional plane strain condition, the dimension along a third axis, x_3// [001], is taken to extend infinitely. Then the model 2 dimensional system may be displayed in terms of x_1, and x_2 coordinates, which are parallel to [100] and [010], respectively.

Voorhees *et al.* [11] formulated the time evolution of the coherent particle. The merit of this method is that the elastic displacement field needs to be evaluated only along the interface. In the present study, the formulation will be briefly summarized. We introduce an atomic misfit or transformation strain, e^{T}_{ij}, and take the reference state for the stress and strain to be the unstrained substrate state. Then the strain tensors for the substrate, e^{S}_{ij}, and film, e^{f}_{ij}, are given by,

$$e^{S}_{ij} = e^{c}_{ij} \tag{1a}$$
$$e^{f}_{ij} = e^{c}_{ij} - e^{T}_{ij} \tag{1b}$$

Where the superscript, c refers to the constrained state, and in this case refers to the strain created when the tractions along the interface are relaxed. The boundary condition for the coherent silicide/Si interface is that the traction and displacement components are continuous across the interface. For the present system, the driving

force consists of two terms, elastic strain and capillarity. The diffusion potential, M, along the interface is then given by,

$$\Gamma M = \Omega\ [||\sigma_{ij}e_{ij}||/2 - \sigma^{S}_{ij}n_j \cdot ||u^{c}_{i,k}n_k|| + \gamma K] \qquad (2)$$

where Γ is the difference in mass densities between two phases, Ω is the atomic volume, $||f|| = f^f - f^S$, refers to the jump property across the interface, n_i is the interface unit normal vector, γ is the energy of silicide/Si interface which is taken to be isotropic and independent of stress, and K is the mean curvature of the film. The potential may be evaluated once the displacement, and its gradient is determined, which is done by applying Green's function method. The elastic strain energy of the system, W, is then given by, $W = -(1/2)[\sigma^{f}_{ij}e^{T}_{ij}]\ dV$, where V is the volume of the film. The total system energy, E, is the sum of elastic strain energy, W, and interfacial energy, S, and is given by, $E = W + S$, where $S = \gamma A$, and A is the interfacial area. For the interface diffusion kinetics, the normal growth rate, v_n, of the film interface according to the potential given by equation (2) is obtained by taking divergence of the atomic flux,

$$v_n = [D\nu\Omega^2/kT](\partial^2\Gamma M/\partial s^2) \qquad (3)$$

where D is the diffusivity, ν is the number of diffusing atoms per unit area, k is Boltzmann constant, T is temperature, and ∂s is the interface arc increment. In the finite-difference formulation, the entire quantities are transformed into the respective dimensionless forms. This is done by employing a standard length, R, which is taken to be the equivalent radius of the semi-circular silicide film. The diffusion potential in its dimensionless form, m, is given by,

$$m = \Lambda[||\sigma_{ij}e_{ij}||/2 - \sigma^{S}_{ij}n_j \cdot ||u^{c}_{i,k}n_k||]/(C_{44}\varepsilon^2) + \kappa \qquad (4)$$

where, ε and κ denote a non-zero component of ε^{T}_{ij}, and the dimensionless interface mean curvature, respectively. The dimensionless parameter, Λ, refers to the elastic strain intensity relative to the capillary force, and is given by equation (5),

$$\Lambda = C_{44}\varepsilon^2 R/\gamma \qquad (5)$$

Equation (5) dictates that the elastic strain intensity scales with the film size, R. It is obvious in equation (4) that diffusion potential takes only the term involving capillary force when Λ vanishes. For $CoSi_2$ film with R scales from 30 to 10 nm, Λ changes from 10 to 3 when $\gamma = 20\ mJ/m^2$ is assumed. Another important dimensionless parameter is the numerical evolution time, τ, which is defined as,

$$\tau = \partial t D\delta\Omega\gamma/[R^4 kT] \qquad (6)$$

where ∂t is the increment in actual time, δ is the thickness of the interface layer. Since τ is inversely proportional to R^4, the scaling of the film size with the factor 0.7 provides the shape evolution kinetics approximately 4 times faster. The detailed finite-difference formulation for the shape evolution problem is described elsewhere [18, 19].

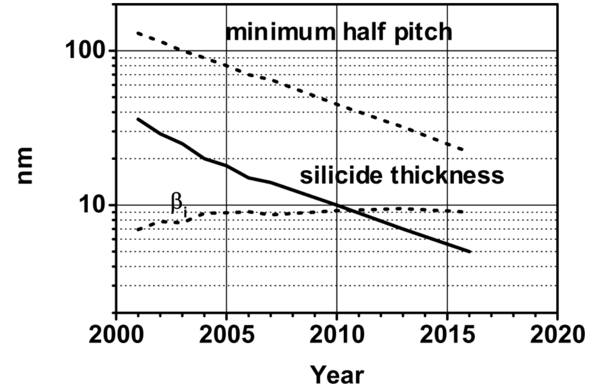

Fig. 1. Semiconductor technology roadmap showing scaling trend for the integrated circuit devices. The minimum feature size and thickness and aspect ratio, β_i, of the silicide film for metal to Si contacts are depicted. The thickness trend also applies to the drain junction application [1]. The β_i is calculated based on the assumptions that there is no silicide material change, and that the contact size for the starting year, 2001 is 250 nm.

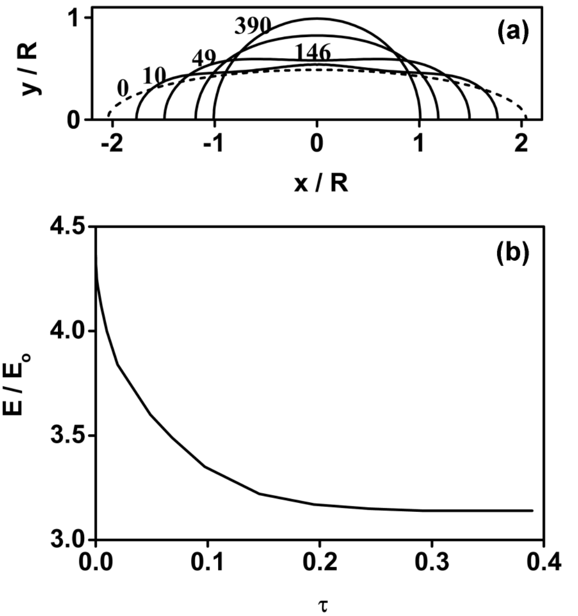

Fig. 2. Shape evolution of a film when only the capillary force is present ($\Lambda = 0$) : (a) time evolution of the film morphology where x and y coordinates are normalized by the standard length, R. The initial aspect ratio of the semi-elliptical film, β_i, is 8.4 and is displayed by a broken line. The evolution times are displayed in terms of normalized unit, $10^{-3}\ \tau$. (b) the normalized system energy vs. time.

3. Results and Discussion

In the results, x_1 and x_2 axes are conveniently denoted by x and y, respectively, and are normalized by R. Since y = 0 is the mirror plane, and refers to the silicide/liner metal interface, the upper half of the film ($y \geq 0$) will only be displayed. Fig. 2 shows the shape evolution of the film for $\Lambda = 0$. Referring to the silicide film aspect ratio for contacts in Fig. 1, the initial shape is taken to be the semi-elliptical shape with $\beta_i = 8.4$, and is denoted by the broken line in Fig. 2(a). As τ increases, the initially flat film evolves to become a semi-circle at τ = 0.390, which is the equilibrium shape for isotropic γ. The system energy, E, normalized by $E_o = \gamma R^2$ is depicted in (b) as a function of time. In Fig. 3, the shape evolution of the film is depicted for (a) $\Lambda = 2$, (b) $\Lambda = 5$, and (c) $\Lambda = 10$, when the dilatational atomic misfit is employed, i.e., $e_{11}^T = e_{22}^T = \varepsilon$ with all other components vanishing. For each case, the shape at largest τ reaches the equilibrium. As Λ increases, the sharp corners start to build up along the elastically hard <110>, and the equilibrium aspect ratio, β_e increases as well. The habit plane is (010) in this case. The system energy vs. time for $\Lambda = 5$ is shown in (d), where the total energy, E decreases to a minimum although the increase in the elastic strain energy W is observed. W is normalized by $W_o = C_{44}\varepsilon^2$. Figure 4. depicts the shape evolu-

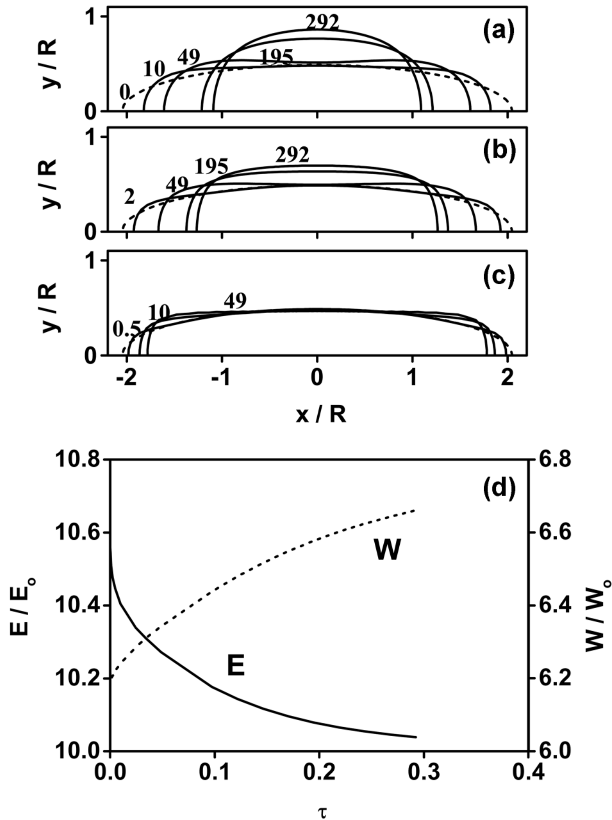

Fig. 3. Shape evolution of the film when the dilatational atomic misfit is employed. The time evolution of the film shape is depicted for (a) $\Lambda = 2$, (b) $\Lambda = 5$, and (c) $\Lambda = 10$. The normalized total system energy, E, and elastic strain energy, W, vs. time for (b) are shown in (d). The evolution times in (a)-(c) are displayed in terms of normalized unit, 10^{-3} τ. The film habit plane is the elastically soft (010).

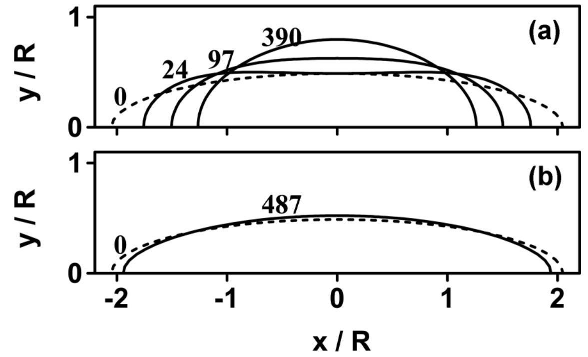

Fig. 4. Shape evolution of the film when the tetragonal atomic misfit along [010] are employed. The time evolution of the film shape is depicted for (a) $\Lambda = 2$, and (b) $\Lambda = 10$. The evolution times are displayed in terms of normalized unit, 10^{-3} τ. The film habit plane is (010) in order to accommodate the misfit.

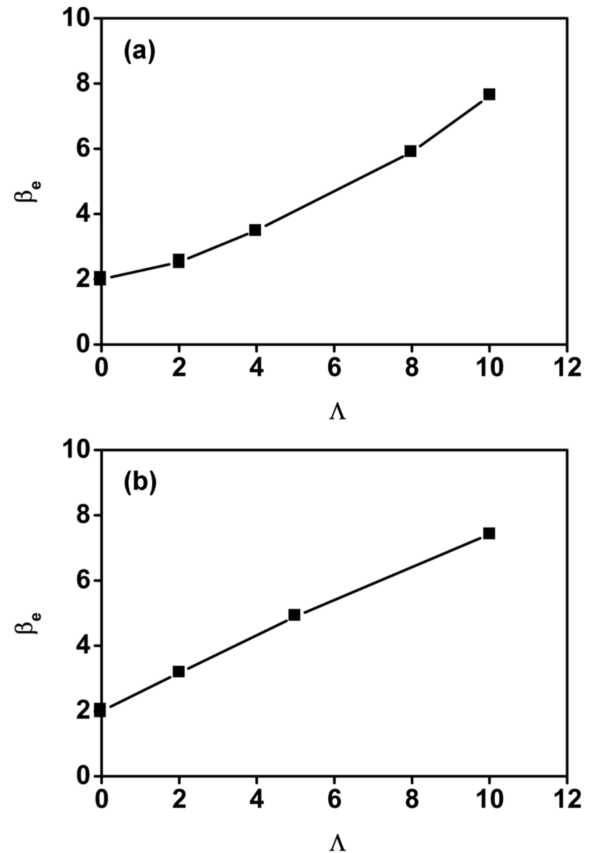

Fig. 5. Equilibrium aspect ratio of the film, β_e, as a function of Λ. (a) dilatational misfit, and (b) tetragonal misfit employed in Figs. 3 and 4, respectively.

tion of the film when the tetragonal atomic misfit along [010] are employed for (a) Λ = 2, and (b) Λ = 10. In this case, $e^T_{22} = \varepsilon$ is the only non-zero component. The equilibrium shape is the one extending along [100] in order to accommodate the misfit, and is given by the shape at largest τ for each case. In Fig. 5, the equilibrium aspect ratio, β_e, of the film is depicted as a function of Λ for both (a) dilatational misfit, and (b) tetragonal misfit cases employed in Figs. 3 and 4, respectively. For both cases, β_e is as large as 8, and is close to β_i when Λ = 10, and decreases to β_e = 2, denoting a semi-circle when Λ decreases to 0. The results state that the flat film with a large aspect ratio is stable at large Λ, but becomes increasingly unstable and eventually shrinks to a shape with small aspect ratio as Λ, or film size decreases. The effect of scaling is clearly shown in Fig. 6, where for the dilatational misfit case, the relative film size and shape profile for Λ = 2, 5 and 10 are depicted in (a). For each case, only the initial (broken line, β_i = 8.4) and equilibrium (solid line) shapes are displayed. As the film size scales, β_e scales as well, and results in the larger area decrease. The percent decrease in film/silicon contact area is depicted in (b) as a function of Λ. When the results are combined with kinetic time scaling as shown in equation (6), the device scaling not only accelerates the agglomeration kinetics, but also increases the reduction in the contact area of the silicide film upon thermal treatment, further deteriorating the electrical performances of the contacts. The former may be alleviated by reducing the thermal budget, while the latter, being the elastic strain-induced effect, may not have the known solution.

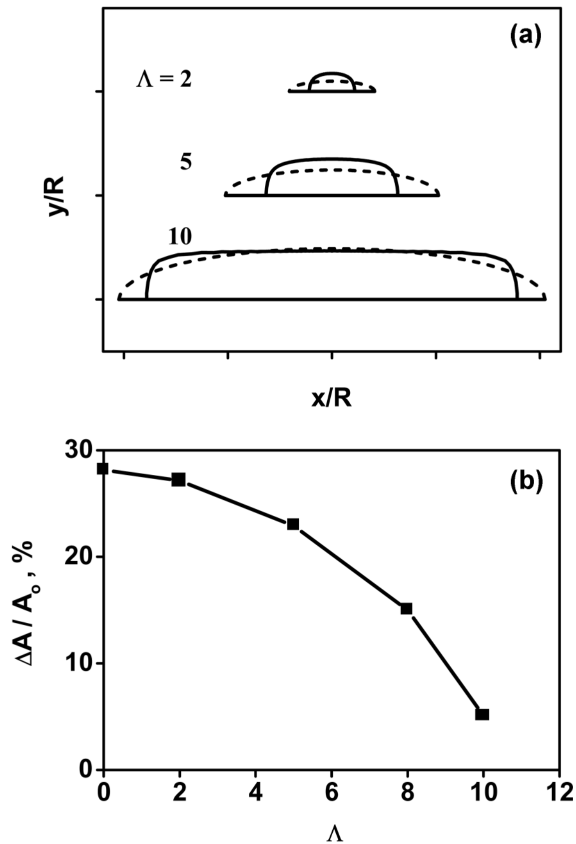

Fig. 6. The effect of device scaling on the film agglomeration when dilatational misfit is employed : (a) the relative film size and shape profile for Λ = 2, 5, 10. The initial (β_i = 8.4) and equilibrium shapes are displayed by broken and solid lines, respectively. (b) The percent decrease in film/silicon contact area as a function of Λ.

4. Conclusions

A new potential problem associated with silicide contacts is identified as the devices for integrated circuit scales. The elastic strain effects on the evolution of the epitaxially grown silicide film are simulated employing continuum linear elasticity and the variational approach. When the atomic misfit is chosen so that the film habit plane is parallel to the film/Si interface, the equilibrium aspect ratio of the film is proportional to the elastic strain intensity, which scales with film size. When the device scaling trend is taken into account, the results show that the flat silicide film shape becomes increasingly unstable to thermal treatment, and may cause to further deteriorate the electrical performance of the contacts, as the film size scales.

References

[1] Semiconductor Industry Association, "International technology roadmap for semiconductors 2002 update", (Semiconductor Industry Association, 2002).

[2] Y. Kim, J. Kim, J. Choy, J. Park and H. Choi, "Effects of cobalt silicidation and post annealing on void defects at the sidewall spacer edge of metal-oxide-silicon field-effect transistors", Appl. Phys. Lett. 75 (1999) 1270.

[3] J. Kim, Y. Kim and J. Choy, "Effects of Ti and TiN capping layers on cobalt-silicided MOS device characteristics in embedded DRAM and logic", J. Korean Cer. Soc. 38 (2001) 782.

[4] S.P. Murarka, "Silicides for VLSI applications" (Academic press, Orlando, 1983) p.30.

[5] J. Choy, Y. Kim, T. Hwang, Y.C. Kim, D. Lee, J. Choi, K. Park and S. Han, "Anomalous scaling effect of tungsten/titanium nitride/titanium to silicon electrical contact resistance for giga bit DRAM applications", J. Electron. Mater. 30 (2001) 1609.

[6] H. Ishiwara, S. Saitoh and K. Hikosaka, "Theoretical

considerations on ion channeling effect through silicide-silicon interface", Japan. J. Appl. Phys. 20 (1981) 843.

[7] A. Londergan, G. Nuesca, C. Goldberg, G. Peterson, A. Kaloyeros, B. Arkles and J. Sullivan, "Interlayer mediated epitaxy of cobalt silicide on silicon (100) from low temperature chemical vapor deposition of cobalt", J. Electrochem. Soc. 148 (2001) C21.

[8] K. Ishida, Y. Miura, K. Hirose, S. Harada and T. Narusawa, "Epitaxial growth of CoSi2 on hydrogen-terminated Si(001)", Appl. Phys. Lett. 82 (2003) 1842.

[9] K. Kim, J. Lee, D. Seo, C. Choi, S. Hong, J. Koh, S. Kim, J. Lee and M. Nicolet, "Growth of epitaxial C54 TiSi2 on Si(111) substrate by in situ annealing in ultra-high vacuum", J. Appl. Phys. 71 (1992) 3812.

[10] M. Stevens, Z. He, D. Smith and P. Bennett, "Structure and orientation of epitaxial titanium silicide nanowires determined by electron microdiffraction", J. Appl. Phys. 93 (2003) 5670.

[11] P. Voorhees, G.. Mcfadden and W. Johnson, "On the morphological development of second-phase particles in elastically-stressed solids", Acta Metall. Mater. 40 (1992) 2979.

[12] J. Choy and J. Lee, "On the shape evolution of a two dimensional coherent precipitate with a general misfit strain", Mater. Sci. Eng. A285 (2000) 195.

[13] K. Thornton, J. Agren and P. Voorhees, "Modelling the evolution of phase boundaries in solids at the meso- and nano-scales", Acta Mater. 51 (2003) 5675.

[14] R. Hill, "The elastic behavior of a crystalline aggregate", Proc. Phys. Soc. London A 65 (1952) 349.

[15] M. Karimi, H. Yates, J. Ray, T. Kaplan and M. Mostoller, "Elastic constants of silicon using monte carlo simulations", Phys. Rev. B 58 (1998) 6019.

[16] G. Guenin, M. Ignat and O. Thomas, "Determination of the elastic constants of a cobalt disilicide intermetallic compound", J. Appl. Phys. 68 (1990) 6515.

[17] P. Ravindran, L. Fast, P. Korzhavyi and B. Johansson, "Density functional theory for calculation of elastic properties of orthorhombic crystals: application to TiSi2", J. Appl. Phys. 84 (1998) 4891.

[18] F. Nichols and W. Mullins, "Morphological changes of a surface of revolution due to capillarity-induced surface diffusion", J. Appl. Phys. 36 (1965) 1826.

[19] J. Choy, S. Hackney and J. Lee, "Nonlinear stability analysis of the diffusional spheroidization of rods", J. Appl. Phys. 77 (1995) 5647.